Elimination of Aberrations Due to High-Order Terms in Systems Based on Linear Time Lenses

Bo Li and Shuqin Lou

***Abstract*—Signal-processing systems based on linear time lenses are realized by the combination of temporal quadratic phase modulation (which is a time lens) and group-velocity dispersion. In practice, these systems suffer from aberrations due to high-order phase-modulation terms in time lenses and aberrations due to high-order dispersion in dispersive elements. We find that these two kinds of aberrations can counterbalance each other under certain conditions. In this paper we theoretically derive and numerically confirm the aberration-elimination conditions for several time-lens based systems, i.e., temporal imaging, time-to-frequency mapping and frequency-to-time mapping of optical pulse waveforms. In addition, a frequency-time diagram is used to analyze the elimination process in order to illustrate the physical mechanism.**

***Index Terms*—Dispersion, frequency-to-time mapping, temporal imaging, temporal phase modulation, time lens, time-to-frequency mapping.**

I. Introduction

THE space-time duality arises from the equivalence between the paraxial diffraction of a spatial field and dispersive propagation of a temporal field [1]–[3]. The duality implies that spatial optical components such as a lens have temporal counterpart known as a time lens, which can be implemented by applying a temporal quadratic phase shift. Using the mature concepts of spatial-imaging systems, temporal imaging [4], time-to-frequency mapping [5] and frequency-to-time mapping [6] of optical pulse waveforms have been realized by properly combining time lenses and group-velocity dispersion. Time-lens based systems have many applications on ultrafast optical processing and measurement, including waveform time stretching [7], single-shot measurements on a timescale of several tens of picoseconds [8], elimination of linear and nonlinear fiber-propagation impairments [9], and arbitrary waveform generation [10].

A time lens is conventionally implemented by imparting a temporal quadratic phase shift across a signal. It can be realized by linear [4]–[6], [10]–[17] or nonlinear [7]–[9], [18]–[20] processes. In particular, linear time lenses offer important practical advantages over nonlinear implementations, including wavelength-preserving operation, lower power consumption, and easier reconfiguration. Driven by a sinusoidal voltage, electro-optic phase modulators can provide the required quadratic phase modulation, which is based on linear process. However, the time lens based on electro-optic phase modulation suffers from aberrations due to the inevitable high-order phase-modulation terms arising from the deviation of the practical sinusoidal modulation profile and the ideal quadratic modulation profile. Thus, some aberration-correction techniques were proposed to eliminate these aberrations. At the beginning, the aberrations due to high-order phase-modulation terms were efficiently suppressed by adding a correction lens according to the Fourier expansion [10]. This configuration was then improved by the use of only one electro-optic phase modulator driven by first and second harmonics with a suitable ratio [11]. This new configuration is also based on Fourier expansion. In [12], a nonlinear least squares fit was proposed to improve the method based on Fourier expansion, and an aberration-free time lens over a large time window was realized. Time lenses can be also implemented by nonlinear processes as well, for example, cross-phase modulation [9], sum-frequency or difference-frequency generation [7], [18], and four-wave mixing in nonlinear materials [8], [19], [20]. Compared with linear time lenses, nonlinear time lenses are mainly limited by a series of nonlinear effects, which are typically improved by the use of novel platforms, instead of linear high-order terms [20].

On the other hand, time-lens based systems also suffer from aberrations due to high-order dispersion in dispersive elements. The high-order dispersion in dispersive elements can introduce spectral aberrations to a time-lens based system [18]. This situation becomes more serious when the input signal is ultrashort [21]. Fiber Bragg gratings (FBGs) are one way of overcoming these aberrations because FBGs can support nearly ideal dispersion with low high-order dispersion [22]. To improve the reconfigurability, a Fourier-domain programmable optical processor has been also proposed to replace FBGs[19].

However, the above-mentioned methods can only eliminate individual aberrations due to high-order phase-modulation terms in time lenses or high-order dispersion in dispersive elements. An alternative method has been proposed to eliminate the aberrations due to high-order terms (including high-order phase-modulation terms in time lenses and high-order dispersion in dispersive elements) simultaneously [17], [18], [23]. In these reports, the aberration due to high-order phase-modulation terms in time lenses and the aberration due to high-order dispersion in dispersive elements are proposed to counterbalance each other. Previous work has proved that an aberration-free system can be achieved using imperfect time lenses with high-order

Manuscript received April 25, 2012; revised April 15, 2013; accepted May 07, 2013. Date of publication May 13, 2013; date of current version June 14, 2013. This work is supported in part by the National Natural Science Foundation of China under Grants 60977033 and 61177082, in part by the Beijing Natural Science Foundation under Grants 4122063, and in part by the Fundamental Research Funds for the Central Universities under Grant 2012YJS002.

The authors are with the School of Electronic and Information Engineering, Beijing Jiaotong University, Beijing 100044, China (e-mail: 11111024@bjtu.edu.cn; shqlou@bjtu.edu.cn).

Color versions of one or more of the figures in this paper are available online at http://ieeexplore.ieee.org.

Digital Object Identifier 10.1109/JLT.2013.2262670

TABLE I
EQUATIONS MODELING FOR A DISPERSIVE ELEMENT AND A TIME LENS WITH A TIME RAY METHOD.

System element	Equations
A dispersive element	$\tau_{out} = \tau_{in} + \Omega\phi'' + \Omega^2 \frac{\phi'''}{2!} + \Omega^3 \frac{\phi^{(4)}}{3!} + \dots,$ $\Omega_{out} = \Omega_{in}$
A time lens	$\tau_{out} = \tau_{in},$ $\Omega_{out} = \Omega_{in} + \tau\Phi'' + \tau^2 \frac{\Phi'''}{2!} + \tau^3 \frac{\Phi^{(4)}}{3!} + \dots$

phase-modulation terms and imperfect dispersive elements with high-order dispersion. Thus the configuration for the signal-processing system would be simplified. However, these previous reports are limited to the elimination of aberrations due to third-order terms in temporal imaging [17], [18] and fourth-order terms in pulse compression [23].

In this work, we investigate the elimination of aberrations due to both third-order terms and fourth-order terms in three signal-processing systems based on linear time lenses, i.e., temporal imaging, time-to-frequency mapping and frequency-to-time mapping of optical pulse waveforms. We derive the aberration-elimination conditions for these three systems by using the time ray method proposed by V. Bennett [18]. These conditions are then confirmed by numerical simulations. Finally, a frequency-time diagram is used to analyze the elimination process in order to illustrate the physical mechanism [24].

II. THEORY

To investigate the aberrations due to high-order terms, a time ray method was proposed to model the temporal imaging system [18]. In the time ray approach, dispersion and time lenses can be described by the relationship between the input time τ_{in} and the output time τ_{out}, and the relationship between the input frequency Ω_{in} and the output frequency Ω_{out}. The expressions for a dispersive element and a time lens are described in Table I [18]. In Table I, $\phi^{(n)} = \beta^{(n)}\xi$ and $\Phi^{(n)}$ is related to nth spectral phase due to dispersion and nth temporal phase due to a time lens, respectively. Note that $\beta^{(n)}$, ξ, τ, Ω are nth-order dispersion coefficient, normalized length of the dispersive element, normalized time, normalized frequency, respectively.

A. Temporal Imaging

The input signals are usually ultrashort in many temporal imaging systems [4], [7], [18], thus it is reasonable to consider that frequency has a larger impact than that of time. Therefore, in [18] the input signal is proposed to represented as $\Omega_{in} = -\tau_{in}/\phi_1'' + \Delta\Omega$, in which $-\tau_{in}/\phi_1''$ is the frequency propagating through the center of the lens and $\Delta\Omega$ is some frequency offset. In order to introduce the time ray approach, we demonstrate the analytical process of eliminating aberrations due to third-order terms as an example, although this conclusion has been proposed in previous work [18].

A temporal imaging system consists of input dispersive element, time lens, and output dispersive element. According to Table I, the output frequency $\Omega_{L,in}$ and time $\tau_{L,in}$ of the input dispersive element can be modeled by (1) and (2), respectively.

$$\Omega_{L,in} = \Omega_{in}, \tag{1}$$

$$\begin{aligned}\tau_{L,in} &= \tau_{in} + \Omega_{in}\phi_1'' + \Omega_{in}^2 \frac{\phi_1'''}{2!} \\ &= \tau_{in} + \left(-\frac{\tau_{in}}{\phi_1''} + \Delta\Omega\right)\phi_1'' + \left(-\frac{\tau_{in}}{\phi_1''} + \Delta\Omega\right)^2 \frac{\phi_1'''}{2!}.\end{aligned} \tag{2}$$

After propagating through the time lens, the output time $\tau_{L,out}$ and frequency $\Omega_{L,out}$ are given by (3) and (4), respectively.

$$\tau_{L,out} = \tau_{L,in}, \tag{3}$$

$$\begin{aligned}\Omega_{L,out} &= \Omega_{L,in} + \tau_{L,in}\Phi'' + \tau_{L,in}^2 \frac{\Phi'''}{2!} \\ &= -\frac{\tau_{in}}{\phi_1''} + \left(1 + \phi_1''\Phi''\right)\Delta\Omega \\ &\quad + \frac{\phi_1'''\Phi''}{2!}\left(-\frac{\tau_{in}}{\phi_1''} + \Delta\Omega\right)^2 \\ &\quad + \frac{\Phi'''}{2!}\left[\phi_1''\Delta\Omega + \frac{\phi_1'''}{2!}\left(-\frac{\tau_{in}}{\phi_1''} + \Delta\Omega\right)^2\right]^2 \\ &\approx -\frac{\tau_{in}}{\phi_1''} + \left(1 + \phi_1''\Phi''\right)\Delta\Omega \\ &\quad + \frac{\phi_1'''\Phi''}{2!}\left(-\frac{\tau_{in}}{\phi_1''} + \Delta\Omega\right)^2 + \frac{\phi_1''^2\Phi'''}{2!}\Delta\Omega,\end{aligned} \tag{4}$$

where the terms including the product terms $\phi'''\Phi'''$ in (4) are ignored because third-order terms (i.e., ϕ''' and Φ''') are much smaller than second-order terms. Finally, the output frequency Ω_{out} and time τ_{out} of the output dispersive element are obtained as (5) and (6).

$$\Omega_{out} = \Omega_{L,out}, \tag{5}$$

$$\begin{aligned}\tau_{out} &= \tau_{L,out} + \Omega_{L,out}\phi_2'' + \Omega_{L,out}^2 \frac{\phi_2'''}{2!} \\ &= -\frac{\phi_2''}{\phi_1''}\tau_{in} + \left(\phi_1'' + \phi_2'' + \phi_1''\phi_2''\Phi''\right)\Delta\Omega \\ &\quad + \frac{\phi_1'''}{2!}\left(1 + \phi_2''\Phi''\right)\left(-\frac{\tau_{in}}{\phi_1''} + \Delta\Omega\right)^2 \\ &\quad + \frac{\phi_1''^2\phi_2''\Phi'''}{2!}\Delta\Omega^2 \\ &\quad + \frac{\phi_2'''}{2!}\left[-\frac{\tau_{in}}{\phi_1''} + \left(1 + \phi_1''\Phi''\right)\Delta\Omega \right. \\ &\quad \left. + \frac{\phi_1'''\Phi''}{2!}\left(-\frac{\tau_{in}}{\phi_1''} + \Delta\Omega\right)^2 + \frac{\phi_1''^2\Phi'''}{2!}\Delta\Omega^2\right]^2 \\ &\approx -\frac{\phi_2''}{\phi_1''}\tau_{in} + \left(\phi_1'' + \phi_2'' + \phi_1''\phi_2''\Phi''\right)\Delta\Omega \\ &\quad + \frac{\phi_1'''}{2!}\left(1 + \phi_2''\Phi''\right)\left(-\frac{\tau_{in}}{\phi_1''} + \Delta\Omega\right)^2 \\ &\quad + \frac{\phi_1''^2\phi_2''\Phi'''}{2!}\Delta\Omega^2 \\ &\quad + \frac{\phi_2'''}{2!}\left[-\frac{\tau_{in}}{\phi_1''} + \left(1 + \phi_1''\Phi''\right)\Delta\Omega\right]^2,\end{aligned} \tag{6}$$

where the terms including the product $\phi'''\Phi'''$ in (6) are ignored. Based on the relationship between the output signal and the input signal in (6), the magnification factor, imaging condition and aberration terms are given by (7)–(9) , respectively.

$$M = -\frac{{\phi_2}''}{{\phi_1}''}, \tag{7}$$

$$\frac{1}{{\phi_1}''} + \frac{1}{{\phi_2}''} - \frac{1}{{\phi_f}''} = 0, \tag{8}$$

$$\begin{aligned} A_b = \frac{1}{2}\Bigg[& \left({\phi_1}''' - {\phi_1}''^3\Phi''' + \frac{{\phi_2}'''}{\mathrm{M}^3}\right)\Delta\Omega^2 \\ & - 2\left({\phi_1}''' + \frac{{\phi_2}'''}{M^2}\right)\frac{\tau_{in}}{{\phi_1}''}\Delta\Omega \\ & + \left({\phi_1}''' + \frac{{\phi_2}'''}{M}\right)\left(\frac{\tau_{in}}{{\phi_1}''}\right)^2\Bigg], \end{aligned} \tag{9}$$

where $\phi_f'' = -1/\Phi''$ is the focal group-delay dispersion associated with the time lens. Equations (7) and (8) are well-known results for temporal imaging [4], which can confirm the above results. Since the input signals in temporal imaging systems are ultrashort, the aberration-elimination condition is obtained as

$${\phi_1}''' - {\phi_1}''^3\Phi''' + \frac{{\phi_2}'''}{\mathrm{M}^3} = 0. \tag{10}$$

Besides third-order phase-modulation terms, the main aberration in time lenses based on electro-optic phase modulation is due to fourth-order phase-modulation terms [4], [10], [12]. Inspired by the pulse compression results in the previous work [21], [23], we find that the aberrations due to fourth-order terms can be also eliminated by each other in time-lens based systems. Using the time ray method, the output time of the temporal imaging system can be obtained as

$$\begin{aligned} \tau_{out} = & M\tau_{in} + \left({\phi_1}'' + {\phi_2}'' + {\phi_1}''{\phi_2}''\Phi''\right)\Delta\Omega \\ & + \frac{M{\phi_1}^{(4)}}{3!}\left(-\frac{\tau_{in}}{{\phi_1}''} + \Delta\Omega\right)^3 \\ & + \frac{{\phi_1}''^3{\phi_2}''\Phi^{(4)}}{3!}\Delta\Omega^3 + \frac{{\phi_2}^{(4)}}{3!}\left(-\frac{\tau_{in}}{{\phi_1}''} + \frac{\Delta\Omega}{M}\right)^3. \end{aligned} \tag{11}$$

Therefore, the aberration-elimination condition is given as

$$M{\phi_1}^{(4)} + {\phi_1}''^3{\phi_2}''\Phi^{(4)} + \frac{{\phi_2}^{(4)}}{M^3} = 0. \tag{12}$$

B. Time-to-Frequency Mapping

The time ray method can be also used to model time-to-frequency mapping systems. Because the input signals are usually ultrashort [5], [8], [20], the frequency of input signal can be expressed as $\Omega_{in} = -\tau_{in}/\phi_1'' + \Delta\Omega$, too. The time-to-frequency mapping system consists of a dispersive element followed by a time lens. Therefore, (4) is suitable for time-to-frequency mapping. From (4) we obtain the time-to-frequency mapping factor and the mapping condition [5], [14] as

$$\Omega_{L,out} = -\frac{\tau_{in}}{{\phi_1}''}, \tag{13}$$

$${\phi_1}'' = {\phi_f}''. \tag{14}$$

And the aberration terms are

$$\begin{aligned} A_b = \frac{1}{2}\Bigg[& \left({\phi_1}'''\Phi'' + {\phi_1}''^2\Phi'''\right)\Delta\Omega^2 \\ & - 2{\phi_1}'''\Phi''\frac{\tau_{in}}{{\phi_1}''}\Delta\Omega + {\phi_1}'''\Phi''\left(\frac{\tau_{in}}{{\phi_1}''}\right)^2\Bigg]. \end{aligned} \tag{15}$$

Because the input signals are usually ultrashort, the aberration-elimination condition is given as

$${\phi_1}'''\Phi'' + {\phi_1}''^2\Phi''' = 0. \tag{16}$$

For time-to-frequency mapping systems with fourth-order terms, the output frequency of the system is obtained as

$$\begin{aligned} \Omega_{L,out} = & -\frac{\tau_{in}}{{\phi_1}''} + \left(1 + {\phi_1}''\Phi''\right)\Delta\Omega \\ & + \frac{{\phi_1}^{(4)}\Phi''}{3!}\left(-\frac{\tau_{in}}{{\phi_1}''} + \Delta\Omega\right)^3 + \frac{{\phi_1}''^3\Phi^{(4)}}{3!}\Delta\Omega^3. \end{aligned} \tag{17}$$

And the aberration-elimination condition is given as

$${\phi_1}^{(4)}\Phi'' + {\phi_1}''^3\Phi^{(4)} = 0. \tag{18}$$

C. Frequency-to-Time Mapping

The temporal duration of the input signals in frequency-to-time mapping systems are usually several tens of picoseconds [6], [9], [13]. Thus it is reasonable to consider that time has a larger impact than that of frequency. Therefore, the input signal is represented as $\tau_{in} = -\phi_2''\Omega_{in} + \Delta\tau$ in time and Ω_{in} in frequency, where $-\phi_2''\Omega_{in}$ is the time propagating through the center of the lens and $\Delta\tau$ is some time offset.

The frequency-to-time mapping system consists of a time lens followed by a dispersive element. Using the same analytical method, the output time of the system with third-order terms is obtained as

$$\begin{aligned} \tau_{out} = & -\Omega_{in}\Phi''{\phi_2}''^2 + \left(1 + \Phi''{\phi_2}''\right)\Delta\tau \\ & + \left(-{\phi_2}''\Omega_{in} + \Delta\tau\right)^2\frac{\Phi'''}{2!}{\phi_2}'' \\ & + \left[\left(1 - {\phi_2}''\Phi''\right)\Omega_{in} + \Phi''\Delta\tau\right]^2\frac{{\phi_2}'''}{2!}. \end{aligned} \tag{19}$$

Thus the frequency-to-time mapping factor and the mapping condition are given by (20) and (21) respectively [9], [14].

$$\tau_{out} = {\phi_2}''\Omega_{in}, \tag{20}$$

$${\phi_2}'' = {\phi_f}''. \tag{21}$$

And the aberration terms are

$$\begin{aligned} A_b = & \left(-{\phi_2}''\Omega_{in} + \Delta\tau\right)^2\frac{\Phi'''}{2!}{\phi_2}'' \\ & + \left[\left(1 - {\phi_2}''\Phi''\right)\Omega_{in} + \Phi''\Delta\tau\right]^2\frac{{\phi_2}'''}{2!}. \end{aligned} \tag{22}$$

When the pulse widths of signals are large enough, terms including Ω_{in} can be ignored. Therefore, the aberration-elimination condition is

$${\phi_2}''\Phi''' + {\phi_2}'''\Phi''^2 = 0. \tag{23}$$

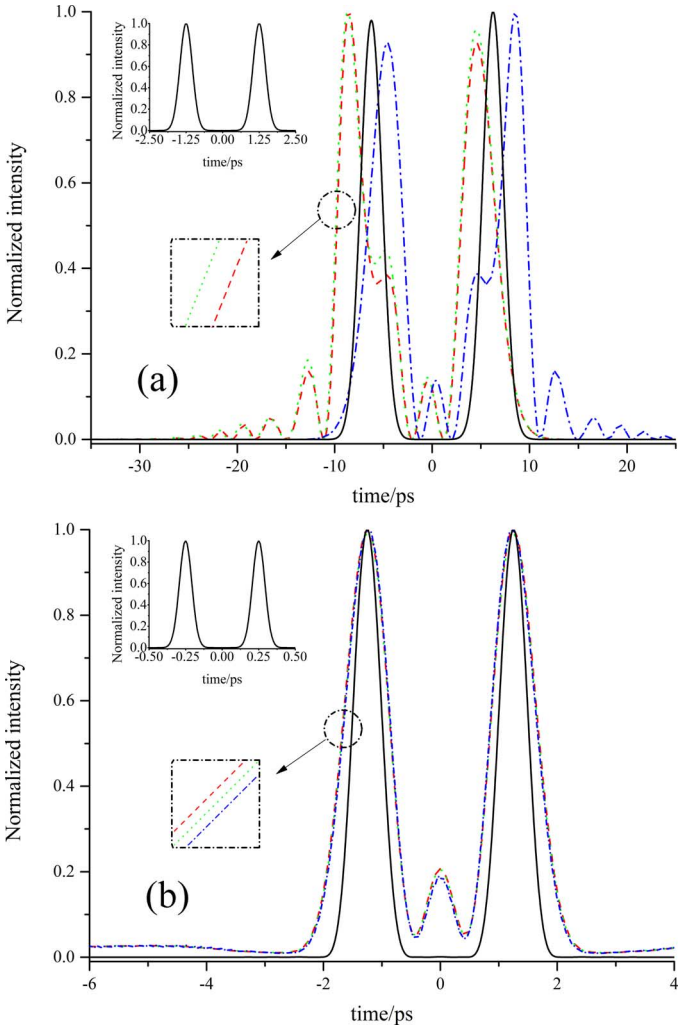

Fig. 1. Temporal intensity profiles (inset) of input waveforms and temporal intensity profiles of output waveforms in temporal imaging systems including nth-order phase-modulation terms in the time lens (blue dash-dotted curve), or nth-order dispersion in the input dispersive element (green dotted curve), or nth-order dispersion in both input and output dispersive elements (red dashed curve), or all nth-order terms (black solid curve). (a) $n = 3$. (b) $n = 4$.

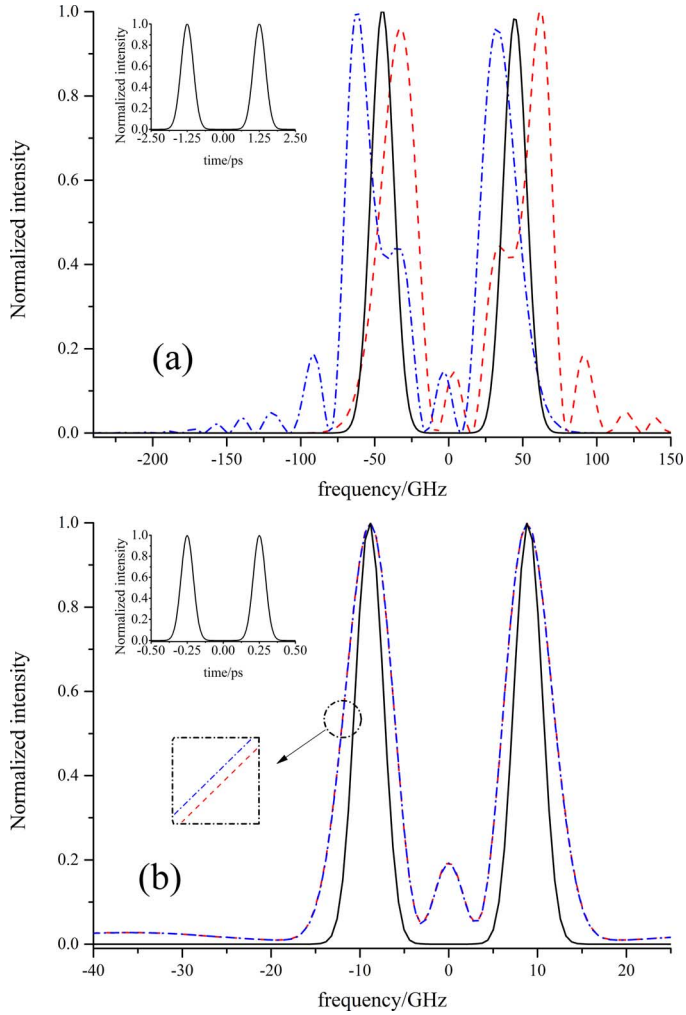

Fig. 2. Temporal intensity profiles (inset) of input waveforms and spectrums of output waveforms in time-to-frequency mapping systems including nth-order phase-modulation terms in the time lens (blue dash-dotted curve), or nth-order dispersion in the dispersive element (red dashed curve), or all nth-order terms (black solid curve). (a) $n = 3$. (b) $n = 4$.

For the frequency-to-time mapping system with fourth-order terms, the output time of the system is

$$\begin{aligned}\tau_{out} = & -\Omega_{in}\Phi''{\phi_2}''^2 + \left(1 + \Phi''{\phi_2}''\right)\Delta\tau \\ & + \left(-{\phi_2}''\Omega_{in} + \Delta\tau\right)^3 \frac{\Phi^{(4)}}{3!}{\phi_2}'' \\ & + \left[\left(1 - {\phi_2}''\Phi''\right)\Omega_{in} + \Phi''\Delta\tau\right]^3 \frac{{\phi_2}^{(4)}}{3!}. \end{aligned} \quad (24)$$

Thus the aberration-elimination condition is

$$\Phi^{(4)}{\phi_2}'' + \Phi''^3{\phi_2}^{(4)} = 0. \quad (25)$$

III. Numerical Simulations and Discussions

Numerical simulations have been done to confirm the analytical results. In Figs. 1–3, we demonstrate temporal intensity profiles or spectrums of the output signals in the above-mentioned systems. In these numerical simulations, all group-velocity dispersion coefficients equal to that of fused silica, i. e. $\beta'' = -27.9\ \mathrm{ps}^2/\mathrm{km}$. In particular, the length of the input dispersive element and magnification factor in Fig. 1 are 1000 m and -5, respectively. The length of the dispersive element in Figs. 2 and 3 are both 1000 m.

Fig. 1 shows the temporal intensity profile of the output waveforms in the temporal imaging systems. The insets are the temporal intensity profiles of the input waveforms. A temporal imaging system consists of input dispersive element, time lens, and output dispersive element. Ideal temporal imaging components must impart a quadratic phase, either spectrally for the dispersive element, or temporally for the time lens modulation. The departure of any realistic component's phase from this idealized form will introduce aberrations in the system [18]. For example, when the third-order dispersion of the input dispersive element and the output dispersive element are both $15.1\ \mathrm{ps}^3/\mathrm{km}$, the corresponding output waveform (red dashed curve) will be distorted, as shown in Fig. 1(a). Compared with the input waveform, the distorted output waveform shifts

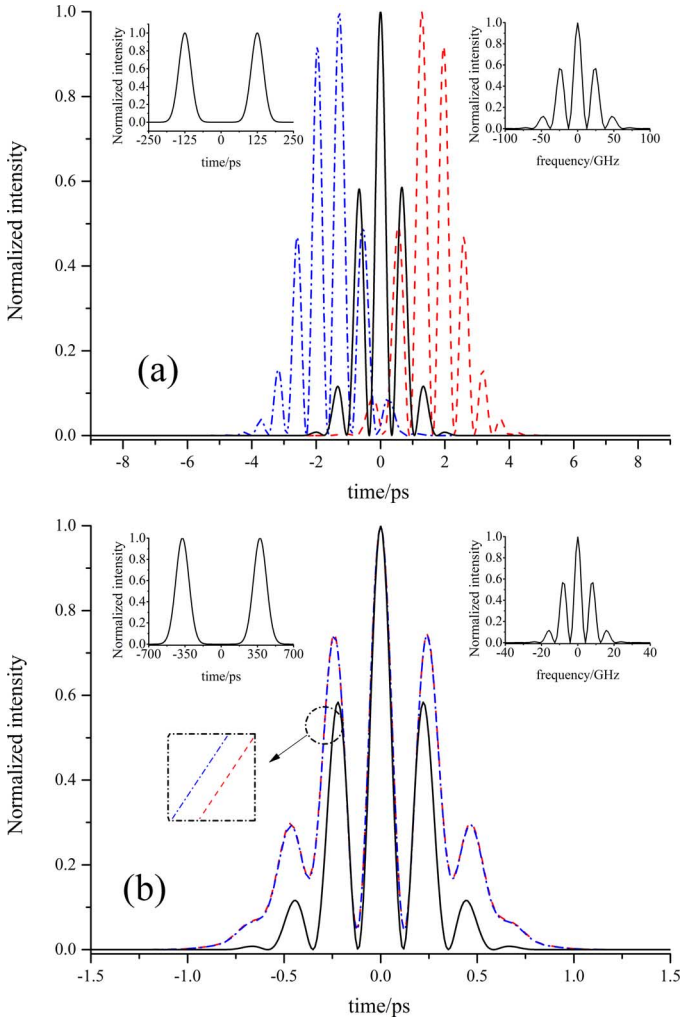

Fig. 3. Temporal intensity profiles (left inset) and spectrums (right inset) of input waveforms and temporal intensity profiles of output waveforms in frequency-to-time mapping systems including nth-order phase-modulation terms in the time lens (blue dash-dotted curve), or nth-order dispersion in the dispersive element (red dashed curve), or all nth-order terms (black solid curve). (a) $n = 3$. (b) $n = 4$.

towards one side and some side-lobes are generated. Then we turn to the investigation of the aberration due to third-order phase-modulation terms in the time lens. Assuming that the dispersive elements are ideal and the time lens has third-order phase-modulation terms (Φ''' is calculated by (10) assuming β''' is 15.1 $\mathrm{ps}^3/\mathrm{km}$), the corresponding output waveform (blue dash-dotted curve) is also distorted, as shown in Fig. 1(a). The distorted output waveform shifts towards the other side and some side-lobes are generated as well. Interestingly, the third-order dispersion and third-order phase-modulation terms introduce aberrations with opposite directions. This result implies that aberrations can be eliminated by the combination of two different aberrations. When the third-order dispersion in dispersive elements and the third-order phase-modulation terms in the time lens are both nonzero, the output waveform (black solid curve) has the same temporal profile as the input waveform except for a magnification factor -5, noting that the aberration-elimination condition is satisfied here. The result confirms our previous theoretical analysis. Note that there are two dispersive elements in the temporal imaging system, thus we further investigate the situation when only the input dispersive element has third-order dispersion. The obtained output waveform (green dotted curve) is similar to the previous one (red dashed curve). It confirms that the input dispersive element plays a dominant role in introducing aberrations for temporal magnification, as predicted in (10). Likewise, Fig. 1(b) demonstrates the aberrations due to fourth-order terms in the temporal imaging system (in which $\beta^{(4)}$ equal to that of fused silica, i. e. 4.9×10^{-4} $\mathrm{ps}^4/\mathrm{km}$). The curves in Fig. 1(b) show that the existence of either the fourth-order dispersion (red dashed curve) or fourth-order phase-modulation terms (blue dash-dotted curve) can introduce aberrations. The output pulses broaden and a center-lobe is generated. When both of fourth-order terms exist and the aberration-elimination condition (12) is satisfied, the aberrations are eliminated and the output waveform has the same temporal profile as the input waveform except for a magnification factor -5.

Fig. 2(a) shows the spectrums of the output waveforms generated in the time-to-frequency systems with third-order terms. Similar to the results shown in Fig. 1(a), the existence of the third-order dispersion (red dashed curve) and third-order phase-modulation terms (blue dash-dotted curve) can introduce aberrations and the distorted waveforms shift to opposite directions. Using the aberration-elimination condition (16), these aberrations are effectively compensated (black solid curve). Fig. 2(b) shows the spectrums of the output waveforms generated in the time-to-frequency systems with fourth-order terms. In particular, the existence of the fourth-order dispersion (red dashed curve) and fourth-order phase-modulation terms (blue dash-dotted curve) can introduce aberrations. The bandwidths of the output pulses broaden and a center-lobe is generated. Using the aberration-elimination condition (18), these aberrations are effectively compensated (black solid curve).

Similar results are also obtained in frequency-to-time mapping, as shown in Fig. 3. Note that the input waveforms are wider than those of Figs. 1 and 2, as a result of our previous assumption. It can be seen from Fig. 3 that aberrations occur due to either third-order terms or fourth-order terms, as shown in Fig. 3(a) and (b), respectively. Moreover, these aberrations are effectively compensated (black solid curve) using the aberration-elimination conditions (23) and (25), respectively.

Next we present the physical mechanism of the proposed method. These processes are readily described with a frequency–time (FT) diagram [24]. In this diagram, dispersion has the effect of shearing the FT line clockwise, and the quadratic phase modulation has the effect of adding the FT lines of input signal with a mixing signal that has a slope of $-1/\tau$ [24]. Due to the similarity of three systems, we take the elimination of aberrations due to third-order terms in time-to-frequency mapping system for an example. The temporal profile and the FT lines of the input signal are represented in Fig. 4(a) and (b), respectively. With the input group-delay dispersion, the FT lines are ideally sheared to a slope of $1/\tau$ (dashed curves) according to the mapping condition (14), as shown in Fig. 4(c). Then the FT lines are mixed with a mixing signal which stands for ideal quadratic phase modulation (dashed curves) as shown in Fig. 4(c) and (d). Based on the diagram, we represent the

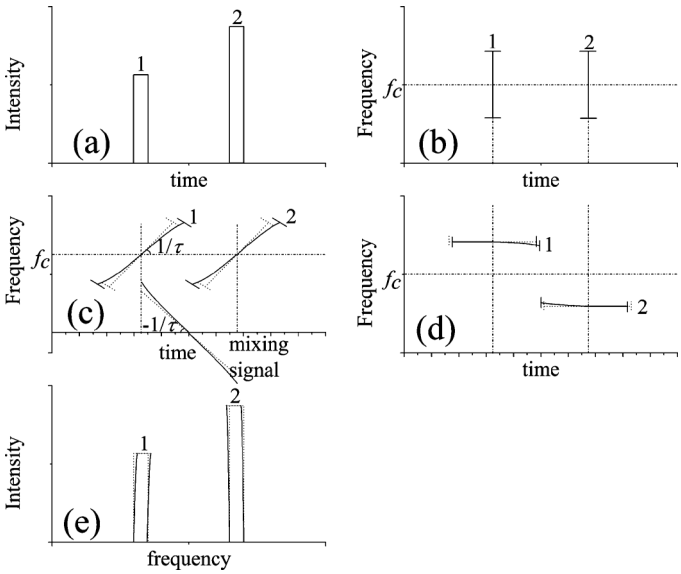

Fig. 4. A time-to-frequency mapping system analyzed by the FT diagram. (a) Temporal profile of the input signal, (b) FT lines of the input signal, (c) FT lines of the dispersed signal and the mixing signal standing for a time lens, (d) FT lines of the output signal, (e) spectrum of the output signal.

effect of third-order dispersion as curving the FT lines (solid curves) and represent the effect of third-order phase-modulation as adding the FT lines with a curved mixing signal (solid curves), as illustrated in Fig. 4(c). The aberration due to third-order dispersion distorts the FT lines to one side in temporal domain, which is confirmed in previous work [18]. Similarly, the aberration due the third-order phase-modulation term distorts the mixing signal to one side in spectral domain. It can be seen from Fig. 4(c) that these two kinds of aberrations can be compensated by the combination of them under a proper condition. And aberrations in the output signal are greatly suppressed (solid curves), as shown in Fig. 4(d) and (e).

In sum, we have investigated the elimination of aberrations due to high-order terms under the aberration-elimination conditions. In practice, these conditions can be satisfied using FBGs or dispersion managed elements, because the high-order dispersion coefficients can be accurately designed [23]. Using a FT diagram, the physical processes of eliminating aberrations are clearly demonstrated. However, the representation is not very accurate as the FT diagram require a time-bandwidth product of > 10 to depict a signal [24]. To get a better description and understanding of the physical processes, joint time-frequency signal representation is a promising tool [22]. Based on joint time-frequency signal representation, every aberration terms in the time ray method could be associated with the practical physical phenomena, and further improvement on the quality of signals could be made. Finally, our method may be potentially used in signal-processing systems based on nonlinear time lenses as well. For example, the resolution of the system based on four-wave mixing is ultimately limited by the aberrations arising from the third-order dispersion [8]. Therefore, there is a requirement for the elimination of aberrations due to high-order terms in signal-processing systems based on nonlinear time lenses.

IV. Conclusion

We have proposed a new method to eliminate aberrations due to third-order terms and fourth-order terms in temporal imaging, time-to-frequency mapping and frequency-to-time mapping systems based on linear time lenses. The proposed method permits one to realize an aberration-free time-lens based system with simple dispersive elements and time lenses, instead of complicated configurations. By using a time ray approach, six corresponding aberration-elimination conditions are obtained. We numerically confirm the aberration-free performance of these systems under the aberration-elimination conditions. Using a FT line diagram, we explain the physical mechanism of the elimination process. In all, our optimization technique is useful for a variety of time-lens based applications, such as ultrafast optical signal process and signals distortion-free transformation.

References

[1] S. Akhmanov, A. Chirkin, K. Drabovich, A. Kovrigin, R. Khokhlov, and A. Sukhorukov, "Nonstationary nonlinear optical effects and ultrashort light pulse formation," *IEEE J. Quantum Electron.*, vol. 4, no. 10, pp. 598–605, Oct. 1968.

[2] A. Papoulis, *Systems and Transforms with Applications in Optics*. New York, NY, USA: McGraw-Hill, 1968.

[3] E. Treacy, "Optical pulse compression with diffraction gratings," *IEEE J. Quantum Electron.*, vol. 5, no. 9, pp. 454–458, Sep. 1969.

[4] B. H. Kolner, "Space-time duality and the theory of temporal imaging," *IEEE J. Quantum Electron.*, vol. 30, no. 8, pp. 1951–1936, Aug. 1994.

[5] M. Kauffman, W. Banyai, A. Godil, and D. Bloom, "Time-to-frequency converter for measuring picosecond optical pulses," *Appl. Phys. Lett.*, vol. 64, no. 3, pp. 270–272, Jan. 1994.

[6] M. Romagnoli, P. Franco, R. Corsini, A. Schiffini, and M. Midrio, "Time-domain Fourier optics for polarization-mode dispersion compensation," *Opt. Lett.*, vol. 24, no. 17, pp. 1197–1199, Sep. 1999.

[7] C. Bennett, R. Scott, and B. Kolner, "Temporal magnification and reversal of 100 Gb/s optical data with an up-conversion time microscope," *Appl. Phys. Lett.*, vol. 65, no. 20, pp. 2513–2515, Nov. 1994.

[8] M. A. Foster, R. Salem, D. F. Geraghty, A. C. Turner-Foster, M. Lipson, and A. L. Gaeta, "Silicon-chip-based ultrafast optical oscilloscope," *Nature*, vol. 456, no. 7218, pp. 81–84, Nov. 2008.

[9] M. Nakazawa, T. Hirooka, F. Futami, and S. Watanabe, "Ideal distortion-free transmission using optical Fourier transformation and Fourier transform-limited optical pulses," *IEEE Photon. Technol. Lett.*, vol. 16, no. 4, pp. 1059–1061, Apr. 2004.

[10] J. van Howe, J. Hansryd, and C. Xu, "Multiwavelength pulse generator using time-lens compression," *Opt. Lett.*, vol. 29, no. 13, pp. 1470–1472, Jul. 2004.

[11] R. Wu, V. R. Supradeepa, C. M. Long, D. E. Leaird, and A. M. Weiner, "Generation of very flat optical frequency combs from continuous-wave lasers using cascaded intensity and phase modulators driven by tailored radio frequency waveforms," *Opt. Lett.*, vol. 35, no. 19, pp. 3234–3236, Oct. 2010.

[12] L. E. Munioz-Camuniez, V. Torres-Company, J. Lancis, J. Ojeda-Castaneda, and P. Andres, "Electro-optic time lens with an extended time aperture," *J. Opt. Soc. Amer. B*, vol. 27, no. 10, pp. 2110–2115, Oct. 2010.

[13] H. Hu, J. L. Areal, E. Palushani, L. K. Oxenlowe, A. Clausen, M. S. Berger, and P. Jeppesen, "Optical synchronization of a 10-G ethernet packet and time-division multiplexing to a 50-Gb/s signal using an optical time lens," *IEEE Photon. Technol. Lett.*, vol. 22, no. 21, pp. 1583–1585, Nov. 2010.

[14] A. W. Lohmann and D. Mendlovic, "Temporal filtering with time lenses," *Appl. Opt.*, vol. 31, no. 29, pp. 6212–6219, Oct. 1992.

[15] A. Godil, B. Auld, and D. Bloom, "Time-lens producing 1.9 ps optical pulses," *Appl. Phys. Lett.*, vol. 62, no. 10, pp. 1047–1049, Mar. 1993.

[16] M. T. Kauffman, A. A. Godil, B. A. Auld, W. C. Banyai, and D. M. Bloom, "Applications of time lens optical systems," *Electron. Lett.*, vol. 14, no. 3, pp. 268–269, Feb. 1993.

[17] V. B. Yurchenko, "Improving the accuracy of a time lens," *J. Opt. Soc. Am. B*, vol. 14, no. 11, pp. 2921–2924, Nov. 1997.

[18] C. V. Bennett and B. H. Kolner, "Aberrations in temporal imaging," *IEEE J. Quantum Electron.*, vol. 37, no. 1, pp. 20–32, Jan. 2001.
[19] J. Schroder, F. Wang, A. Clarke, E. Ryckeboer, M. Pelusi, M. A. F. Roelens, and B. J. Eggleton, "Aberration-free ultra-fast optical oscilloscope using a four-wave mixing based time-lens," *Opt. Commun.*, vol. 283, no. 12, pp. 2611–2614, Jun. 2010.
[20] A. Pasquazi, Y. Y. Park, S. T. Chu, B. E. Little, F. Légaré, R. Morandotti, J. Azaña, and D. J. Moss, "Time-lens measurement of subpicosecond optical pulses in CMOS compatible high-index glass waveguides," *IEEE J. Sel. Top. Quantum Eletrcon.*, vol. 18, no. 2, pp. 629–636, Mar. 2012.
[21] M. D. Pelusi, Y. Matsui, and A. Suzuki, "Electrooptic phase modulation of stretched 250-fs pulses for suppression of third-order fiber dispersion in transmission," *IEEE Photon. Technol. Lett.*, vol. 11, no. 11, pp. 1461–1463, Nov. 1999.
[22] J. Azana and M. A. Muriel, "Real-time optical spectrum analysis based on the time-space duality in chirped fiber gratings," *IEEE J. Quantum Electron.*, vol. 36, no. 5, pp. 517–526, May 2000.
[23] G. Deng, W. Pan, and X. H. Zou, "Optical pulse compression using the combination of phase modulation and high-order dispersion compensation," *Opt. Rev.*, vol. 17, no. 5, pp. 454–458, Sep. 2010.
[24] P. Naulleau and E. Leith, "Stretch, time lenses, and incoherent time imaging," *Appl. Opt.*, vol. 34, no. 20, pp. 4119–4128, Jul. 1995.

Bo Li was born in Shandong, China, on November 29, 1989. He received the B. S. degree in applied physics from Shandong University, Jinan, China, in 2009 and the M.S. degree in optical communication from Beijing Jiaotong University, Beijing, China, in 2011. He started to pursue the Ph.D. degree in the same university in 2011, majoring in communication and information system. Under an exchange program (from 2012 to 2014), he is currently working in the Ultrafast Optical Processing group at the Institut National de la Recherche Scientifique–Energie, Matériaux et Télécommunications (INRS-EMT)–Université du Québec, (Montréal, Canada), under the supervision of Prof. José Azaña.

His recent research interests include ultrafast optical signal processing using space-time duality.

Shuqin Lou was born in Hei Longjiang Province, China, in 1965.

She is currently a Professor with the School of Electronic and Information Engineering, Beijing Jiaotong University, Beijing, China. Her current research interests include optical communication, optical signal process, special fiber and fiber device.